AD-A123 234 THE ELECTROMAGNETIC BIAS OF ALTIMETER MEASUREMENTS OF MEAN SEA LEVEL AS D..(U) NAVAL RESEARCH LAB WASHINGTON DC L W CHOY ET AL. 12 JAN 83 NRL-MR-5006 1/1

UNCLASSIFIED F/G 1/4 NL

END

FILMED

DTIC

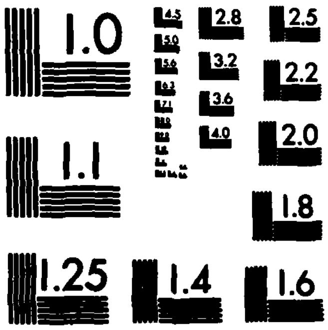

MICROCOPY RESOLUTION TEST CHART
NATIONAL BUREAU OF STANDARDS-1963-A

AD A123234

NRL Memorandum Report 5006

...he Electromagnetic Bias of A... Measurements of Mean Sea L... Determined by an Airborne 10 GHz Radar

L. W. CHOY, D. L. HAMMOND AND E. A. U...

Space Sensing Applications Branch
Aerospace Systems Division

January 12, 1983

This report was funded jointly by NAVAIR, ON...

NAVAL RESEARCH LABORATORY
Washington, D.C.

83 1 11 003

SECURITY CLASSIFICATION OF THIS PAGE (When Data Entered)

REPORT DOCUMENTATION PAGE

READ INSTRUCTIONS BEFORE COMPLETING FORM

1. REPORT NUMBER	2. GOVT ACCESSION NO.	3. RECIPIENT'S CATALOG NUMBER
NRL Memorandum Report 5006	AD-A123234	

4. TITLE (and Subtitle)
THE ELECTROMAGNETIC BIAS OF ALTIMETER MEASUREMENTS OF MEAN SEA LEVEL AS DETERMINED BY AN AIRBORNE 10 GHz RADAR

5. TYPE OF REPORT & PERIOD COVERED
Interim report on a continuing NRL problem.

6. PERFORMING ORG. REPORT NUMBER

7. AUTHOR(s)
L.W. Choy, D.L. Hammond, E.A. Uliana

8. CONTRACT OR GRANT NUMBER(s)

9. PERFORMING ORGANIZATION NAME AND ADDRESS
Naval Research Laboratory
Washington, DC 20375

10. PROGRAM ELEMENT, PROJECT, TASK AREA & WORK UNIT NUMBERS
W05270S00; 63207N; 79-0932-0-0; RR1452-SB1000; 63371N;
(Continues)

11. CONTROLLING OFFICE NAME AND ADDRESS
Naval Air Systems Command
Washington, DC 20360

12. REPORT DATE
January 12, 1983

13. NUMBER OF PAGES
16

14. MONITORING AGENCY NAME & ADDRESS (if different from Controlling Office)

15. SECURITY CLASS. (of this report)
UNCLASSIFIED

15a. DECLASSIFICATION/DOWNGRADING SCHEDULE

16. DISTRIBUTION STATEMENT (of this Report)

Approved for public release; distribution unlimited.

17. DISTRIBUTION STATEMENT (of the abstract entered in Block 20, if different from Report)

18. SUPPLEMENTARY NOTES

This project was funded jointly by NAVAIR, ONR, and NASA.

19. KEY WORDS (Continue on reverse side if necessary and identify by block number)

EM Bias
10 GHz radar
Marine Geodesy
Radar altimeter
Oceanography
Remote sensing
Ocean fronts

20. ABSTRACT (Continue on reverse side if necessary and identify by block number)

> Electromagnetic bias, the small difference that exists between the radar measured mean sea level and the geometric mean sea level is an important issue in high precision satellite altimetry. Present day satellite altimetry has achieved, with SEASAT-1, a precision of 5 cm rms in the range measurement. Future altimeter designs are expected to improve the range measurement precision to 2 cm rms. In order to exploit the capability of these precise radar altimeters for marine geodesy and oceanography, it is necessary to understand and account for all of the known biases in the range measurement. The ⟶ over

(Continues)

DD FORM 1473, 1 JAN 73 EDITION OF 1 NOV 65 IS OBSOLETE
S/N 0102-014-6601

SECURITY CLASSIFICATION OF THIS PAGE (When Data Entered)

10. Program Element, Project, Task Area and Work Unit Numbers (Continued).

79-1579-0-0; ~~NASA P-81, 235~~; 79-1401-0-0

20. Abstract (Continued)

electromagnetic bias or the EM bias, which has been attributed to the observed fact that ocean wave troughs tend to be better reflectors of nadir viewing microwave radar energy than ocean wave crests, can be observed with high resolution airborne radar. This report presents the results of the EM bias measurements made by NRL using an airborne radar altimeter operating at 10 GHz with a 1 ns range resolution. Data were taken for various sea states and wind conditions. The experimental results are compared with current theories.

Contents

THE ELECTROMAGNETIC BIAS OF ALTIMETER MEASUREMENTS OF MEAN SEA LEVEL AS DETERMINED BY AN AIRBORNE 10 GHz RADAR

INTRODUCTION

Satellite radar altimetry has matured greatly since the S-193 microwave experiment on SKYLAB ten years ago. For geodesy and oceanography, accurate radar altimeter data are needed for mapping of the marine geoid, ocean currents, and mesoscale features. While the radar altimeter is a range measuring device, ocean wave heights and wind speeds at the sea surface are also obtained with proper analysis of the data. However, measurement of range to high accuracy in the presence of ocean waves is not problem free. The diameter of the footprint illuminated by a satellite-borne radar altimeter is large compared with the lengths of the ocean wind waves. For example, the pulse-width-limited footprint of the SEASAT altimeter had a diameter of 1.6 km for smooth seas. The large footprint effectively acts as a spatial filter (Figure 1) that averages the height of many waves; thus the amplitudes of ocean waves do not directly enter into the range measurement. However, it has been observed (Yaplee, et al, 1971; Shapiro, et al, 1972; Kenney and Walsh, 1978; Choy and Uliana, 1980) that wind generated ocean wave troughs tend to reflect nadir incident microwave signals better than the wave crests. Since a radar altimeter determines its range by measuring the round trip time of a pulse of electromagnetic energy to the sea surface, and uses the centroid of the pulse as the time reference, the range so derived tends to be biased toward the troughs. If we define mean sea surface as the centroid of the wave height distribution, we see that the radar determined "mean" sea surface may not be the same. The difference has been called the electromagnetic bias or the EM bias. To achieve a range accuracy of a few centimeters with spaceborne altimetry, understanding the EM bias problem is important.

The first experiment to investigate the EM bias was reported by Yaplee, et al (1971). Their radar measurements were taken from a navigation tower off the coast near Norfolk, Virginia. Only two cases were reported with low to moderate wave heights. Later reports on EM bias used data collected by airborne sensors with a wider range of wave heights (Kenney, et al, 1979; Choy and Uliana, 1980). There have also been reports on estimates of EM bias using data from satellite-borne radar altimeters (Lipa and Barrick, 1980; Born, et al, 1982;). Theoretical ocean wave models which explain the EM bias have also been reported (Jackson, 1979; Lipa and Barrick, 1980). Comparisons among various observations and observations with theories indicate that the EM bias question is not completely resolved. The present investigation is part of a joint program between NRL and NASA (GSFC/WFC) to address this EM bias problem.

Manuscript approved December 1, 1982.

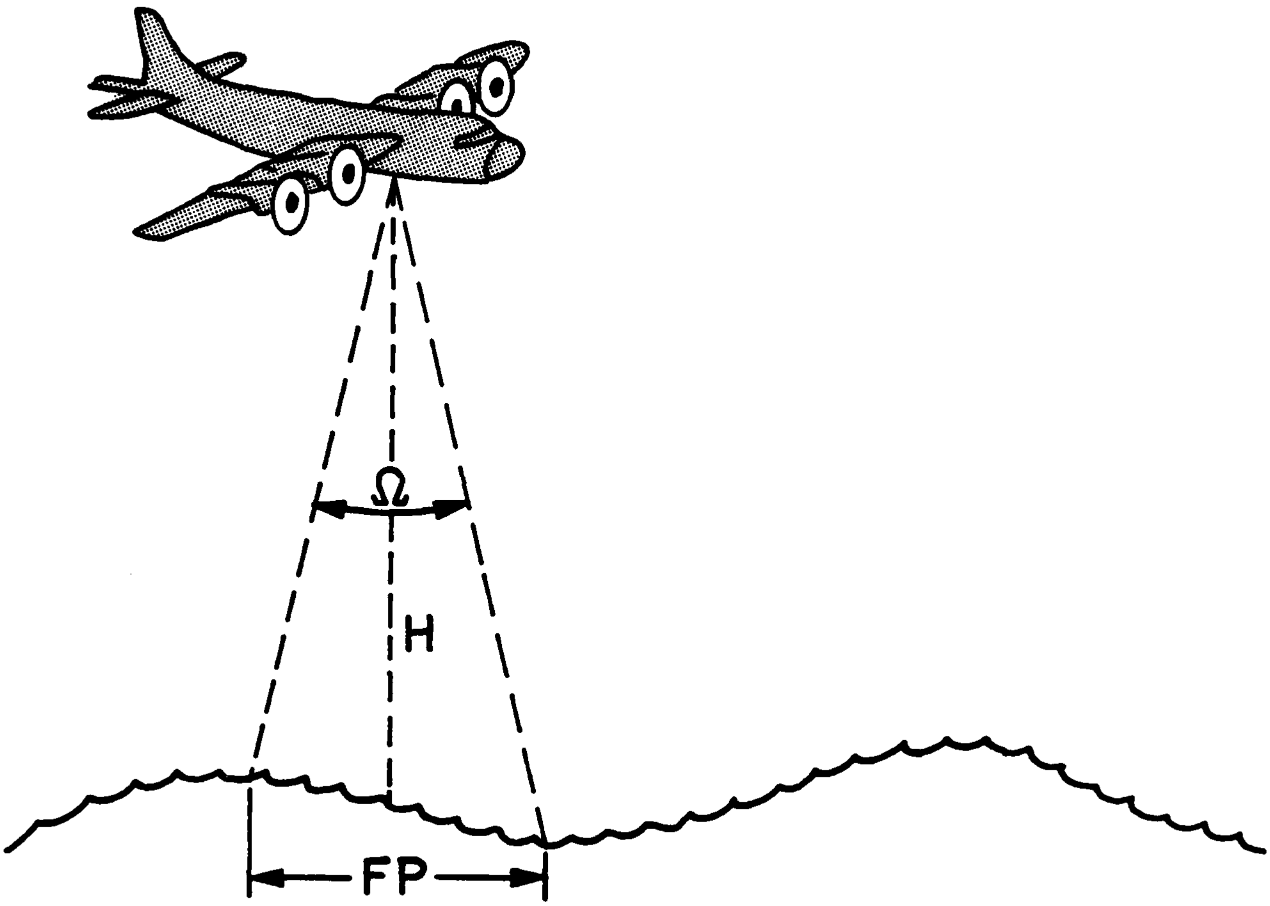

RADAR ALTIMETER GEOMETRY ILLUSTRATING THE SPATIAL FILTERING

H = HEIGHT OF ALTIMETER

Ω = ANGULAR BEAM WIDTH OF ALTIMETER

FP = ALTIMETER FOOTPRINT OR SPOT SIZE ON THE OCEAN SURFACE

Figure 1 - Radar Altimeter Geometry Illustrating Spatial Filtering

THEORETICAL BASIS FOR THE EXPERIMENT

The airborne radar altimeter views the ocean in the nadir direction and measures the ocean surface elevation profile and the backscattered radar power. From these measurements, one can construct the probability density function of the ocean surface elevations and the radar surface impulse response, both quantities as functions of vertical ocean wave displacement relative to the displacement mean. The difference between the mean values of the probability density function of the ocean surface elevations and the radar surface impulse response is defined as the electromagnetic range bias (EM bias) of the altimeter. The radar energy is confined to a narrow pulse (1 ns) illuminating the ocean surface with a footprint which is small relative to the dominant ocean wavelengths encountered. A software radar altimeter range tracker is constructed to track on the centroid or the mean value of the return power. Thus, the probability density of the surface elevations can be approximated by the ratio of the number of pulses received for a given range resolution cell to the total pulses received, and the radar surface impulse response is approximated by the ratio of the average backscattered power in a range cell to the total power received (Figure 2).

Higher moments of the wave elevation distribution (rms wave height, skewness, and kurtosis) can be obtained from the probability density function after carefully removing the contamination of the aircraft motion from the data. However, due to the finite illuminated footprint of the radar altimeter, the values of the moments are underestimated by the spatial filtering effect. The numerical reduction in the estimated values of the variance and skewness of the wave height distribution can be calculated to a first order by using a simple Phillips spectral model F(K) for the water waves (Jackson, 1979).

$$\mu_{20} = \int_{K_o}^{nK_o} F(k)\, dk$$

$$\mu_{30} = \int_{K_o}^{nK_o} F(k) \left[\int_{K_o}^{k} mF(m)\, dm \right] dk$$

$$\lambda_{30} = \frac{\mu_{30}}{\mu_{20}^{3/2}}$$

$$F(K) = \beta K^{-3} \qquad K_o < K < \infty$$

where

$K_o = 2\pi/L$ is the dominant wave number and L is the dominant wavelength.

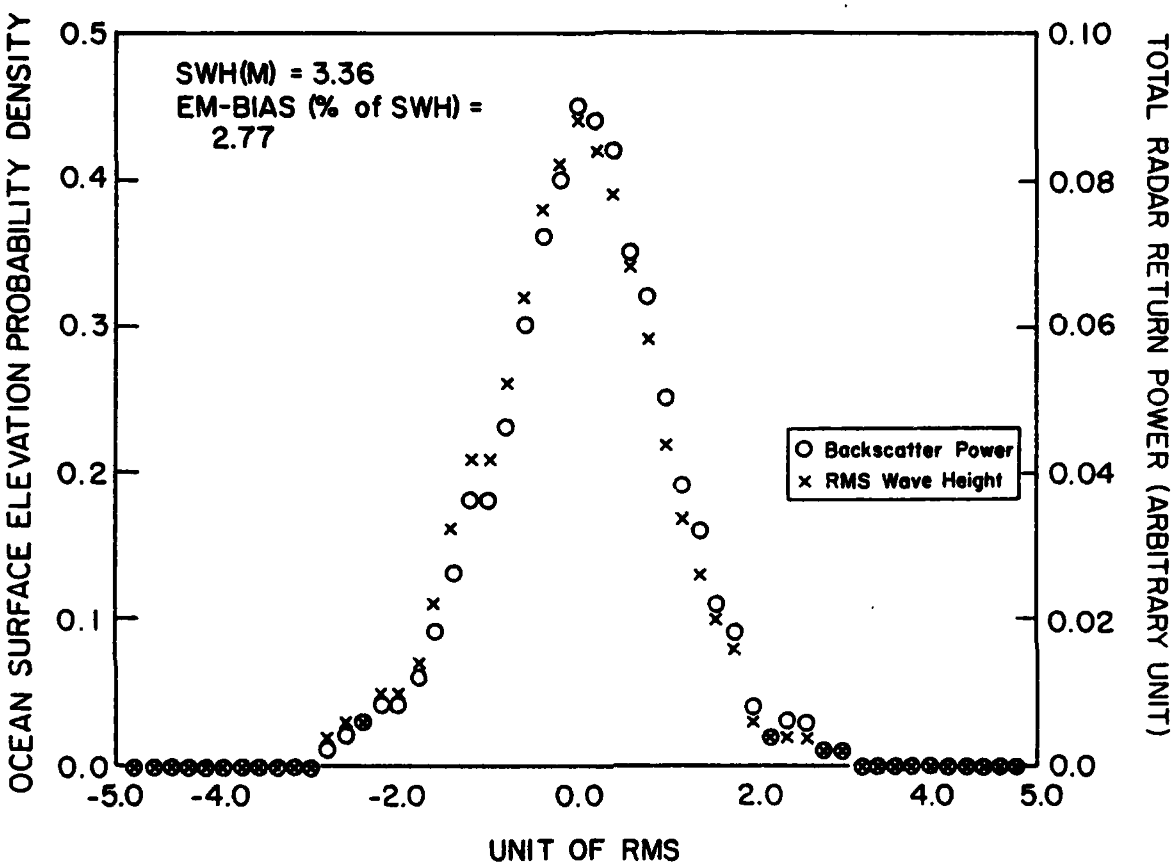

Figure 2 - Ocean surface elevation probability density compared with EM impulse response

μ_{20} is the variance of the wave height probability density.

μ_{30} is the third moment of the wave height probability density.

λ_{30} is the normalized skewness.

nK_o represents the high frequency cut off due to the radar footprint diameter and is equal to $2\pi/D$.

D is the footprint diameter.

Carrying out the indicated integration, the spatially filtered values are

$$\mu'_{20} = \frac{\beta}{2K_o^2}\left(1 - \frac{1}{n^2}\right)$$

$$\mu'_{30} = \frac{2\beta^2}{K_o^3}\left(1 - \frac{3}{n^2} + \frac{2}{n^3}\right).$$

It can be seen that when n is large, more of the high frequency waves contribute and both μ'_{20} and μ'_{30} approach $\beta/2K_o^2$ and $2\beta^2/K_o^3$, the unfiltered values of μ_{20} and μ_{30}, respectively.

The upper limit of integration is equated with the wave number whose wavelength equals the footprint diameter D. It follows that n is the ratio of dominant wavelength to footprint diameter.

$$\frac{n2\pi}{L} = \frac{2\pi}{D} \text{ or } n = \frac{L}{D}.$$

Since

$$\lambda_{30} = \frac{\mu_{30}}{\mu_{20}^{3/2}}$$

and the filtered

$$\lambda'_{30} = \frac{\mu'_{30}}{\mu'^{3/2}_{20}}$$

or

$$\frac{\lambda'_{30}}{\lambda_{30}} = \frac{\left(1 - \frac{3}{n^2} + \frac{2}{n^3}\right)}{\left(1 - \frac{1}{n^2}\right)^{3/2}}.$$

Table 1 lists the values of μ'_{20}/μ_{20} and $\lambda'_{30}/\lambda_{30}$ for several values of n.

Table 1

The Values of μ'_{20}/μ_{20} and $\lambda'_{30}/\lambda_{30}$ as function of n

n	μ'_{20}/μ_{20}	$\lambda'_{30}/\lambda_{30}$
1	0	--
2	.75	.77
5	.96	.953
10	.99	.987
20	.9975	.996
50	.9996	.9994

The NRL radar altimeter has a footprint diameter about 15 meters for the data used in this report. Thus for ocean surfaces with dominant wavelengths of 75 meters or greater, the reduction in the estimates of variance and normalized skewness is 4 percent or less.

EXPERIMENTAL PROCEDURES

The high resolution radar altimeter antenna and the laser profilometer were mounted near to each other on an airborne platform. The illumination spot of the radar is larger than the laser by a factor of 50 at all altitudes. Both sensors were aligned to look in the nadir direction under stable flying conditions. The sampling rate of the laser is 200 per second. The sampling rate of the radar altimeter can be set on 39 or 78 samples per second. The aircraft ground speed was approximately 100 meters per second. Thus the range profile produced simultaneously by both sensors are along the same sea surface track. The laser, in addition to providing an independent check on the performance of the radar, offers a quantitative look at the spatial filtering effect of the radar. The NRL radar is a 10 GHz, bistatic, CW pseudo-random noise coded system. The antenna beam width of 6° combined with the one nanosecond range resolution assures pulse width limited illumination. The laser profilometer is an IR pulsed laser with a pulse width of 10 ns.

The NRL airborne platform is a Navy P-3 aircraft. It is equipped with an inertial navigation system which includes the monitoring of wind speed and direction. A separate set of sensors are installed in the laser profilometer housing close to the radar altimeter to record pitch, roll, and vertical acceleration information of the aircraft. For most of the data examined, the aircraft motion changed slowly. Of the three motions, pitch, roll, and vertical acceleration, the vertical motion was dominant. Typically, in a three-minute interval, two or three large changes in vertical velocity (approximately 50 cm/sec) can be observed. During stable flight segments vertical velocity of the aircraft was less than 5 cm/sec. The aircraft vertical motion was removed by an algorithm based on double integration of the accelerometer data and high pass filtering.

All data used in this report were taken at altitudes of 500 and 750 feet in three locations, the North Sea, Gulf of Alaska, and the Atlantic Ocean just off the East Coast of the United States. When the aircraft reached the operating altitude, data were taken continuously in 3 to 10 minute intervals and recorded on digital magnetic tape. During one of the data flights reported in this paper the NRL and NASA/Wallops radar systems were flown on the same aircraft. On another data flight reported here the two radar systems, although mounted in separate airplanes, collected data simultaneously at the same location. These experiments conducted with NASA/Wallops were at locations off the east coast of the United States.

DATA ANALYSIS PROCEDURE

Data records were divided into two-minute segments. Altimeter height measurements were computed using a software range tracker which operates on the centroid of the averaged (4 samples) received radar pulse waveform. The backscattered power was determined for each pulse using the total power contained in the averaged (4 samples) waveform. Although other types of range trackers using either the location of the peak amplitude of the waveform or a leading edge threshold value on the waveform were tried, we settled on the centroid tracker because the result obtained with it was more stable. The first two moments of the wave height distribution were computed from height data using standard methods.

$$\mu_{oo} = \frac{1}{N}\sum_{i=1}^{N} h_i \qquad\qquad \mu_{20} = \frac{1}{N-1}\sum_{i=1}^{N}(h_i - \mu_{oo})^2$$

μ_{oo} = first moment

h_i = sample of height

N = number of sample heights

μ_{20} = second moment

The third and fourth moments (skewness and kurtosis) were estimated using an ocean surface elevation density model, Longuet-Higgins (1963).

$$g = \frac{1}{2\pi}\left[\exp\left(-\frac{T^2}{2}\right)\right]\left[1 + \frac{\lambda}{6}\left(T^3 - 3T\right) + \frac{K}{24}\left(T^4 - 6T^2 + 3\right)\right]$$

where

g = probability density of height.

$T = t/\sigma_s$.

t = the height above the mean sea level.

σ_s = the rms wave height.

λ = the skewness of the wave height distribution.

K = the kurtosis of the distribution.

The model is a low order case of a general probability function used by Longuet-Higgins (1963) for a random variable that is weakly nonlinear.

For a given σ_s, parameters λ and K were varied so the model best fits the data in a least square sense. The conventional Chi-square is used to estimate the goodness of fit. The computation of skewness is extremely sensitive to the data noise in the tail ends of the wave height distribution. Data which gave a poor fit to the model also gave unreasonable estimates of skewness if the usual formula from statistics was used.

For the majority of the observations, the radar sampling rate was set at 39/second. For a two-minute segment, the number of data points that went into each determination of EM bias, significant wave height, and skewness of the wave height distribution is over 4000. The dominant wavelength information was derived by taking a one-dimensional power spectrum of the wave profiling data, flying in the upwind or downwind direction. Since we have no other independent method of determining the wave propogation direction, the dominant wavelength values were rough estimates. The wind speed was recorded at the aircraft altitude of 500 ft and no attempt was made to re-scale the wind speed to a value corresponding to the sea surface.

DISCUSSION AND CONCLUSIONS

For significant wave heights (SWH) up to five meters, the value of EM bias increases in proportion to SWH. To facilitate the comparison of EM bias with other ocean surface conditions, the unit of EM bias will be expressed as a percentage of the SWH for this section of the report.

Figure 3 is a plot of EM bias (percentage SWH) vs. SWH. Data that were taken on the same day are represented by the same symbol. For most of the data examined with significant wave height in 1 to 5 m range, the EM bias is between three to five percent of SWH. On one occasion, however, the EM bias was centered at 1.5% of the SWH. On that day, the NRL radar was flying jointly with the NASA/Wallops experiment on the NASA aircraft. The skewness of the wave height distribution was observed to be rather small indicating that the sea was dominated by swell. Since the data are grouped by the day of observation, the error bars were placed only on one representative member of a data group. In general, the EM bias estimates have a standard deviation of about $\pm$ 0.5 percent of SWH. The SWH estimates have standard deviations of about $\pm$ 0.15 x SWH in meters. These uncertainties are due to the limited number of data samples available.

Figure 4 is a plot of the EM bias vs. the skewness of the wave height distribution. It is of interest to compare the regression line of these data with the result of Jackson (1979). Jackson concluded that the EM bias expressed in meters is the product of the skewness times the rms wave height. This relation is shown by the straight line in the figure. The line has a slope of 0.04 and an intercept of zero. The regression line for the data has a slope of 0.03 and an intercept of 0.03. Again only a few representative error bars are shown. These errors were calculated using the relation

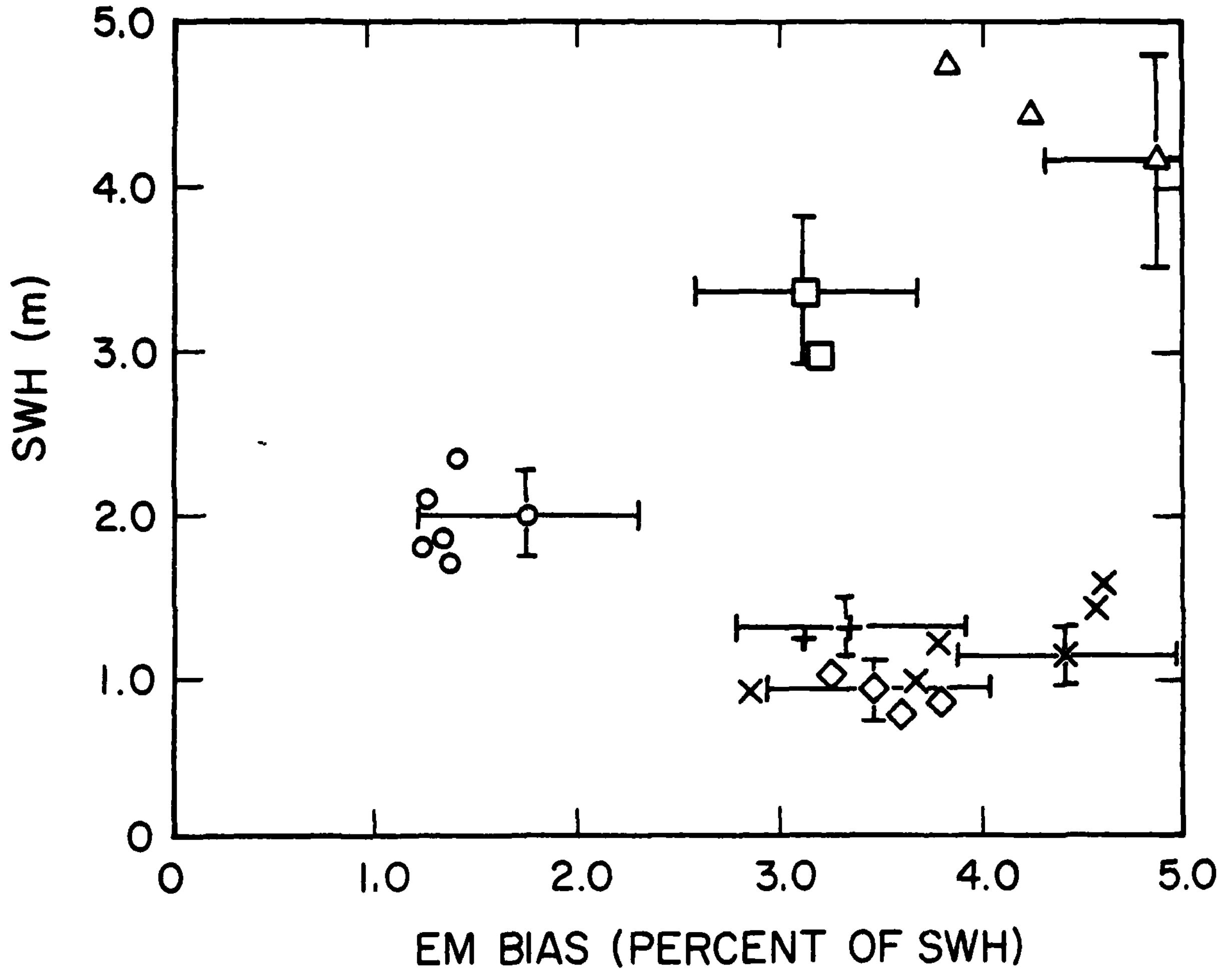

Figure 3 - EM Bias (% SWH) vs. SWH (metric)

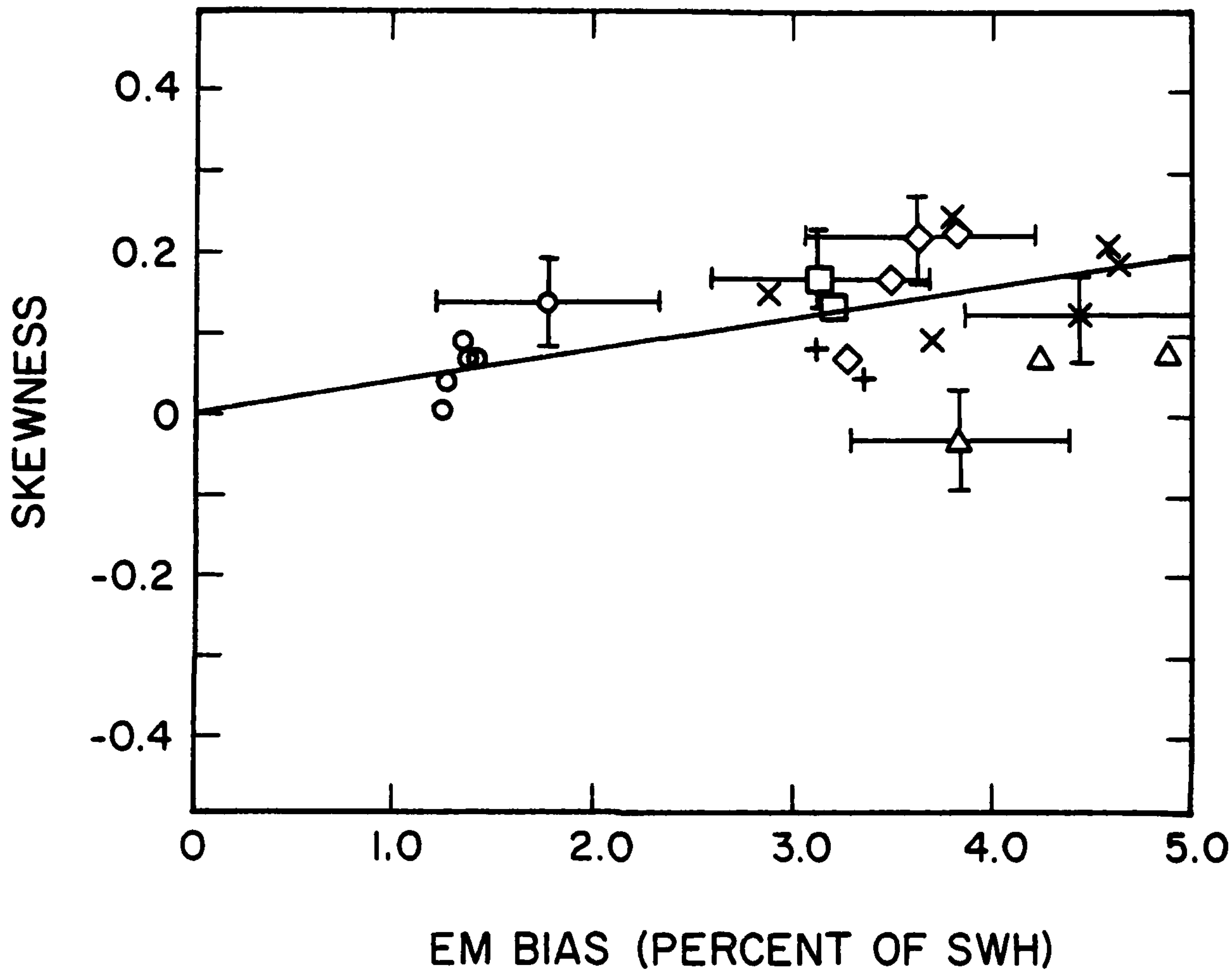

Figure 4 - EM Bias (% SWH) vs. Height Skewness

$$r_a^2 = \frac{\mu_{2a} - \mu_a^2}{N},$$

where

r_a^2 is the mean squared a^{th} moment of the estimation error using N samples,

μ_a is the a^{th} moment of the data samples,

μ_{2a} is the $2a^{th}$ moment of the data samples, and

N is the number of independent samples.

The number of data samples were on the order of 4000 for every point. The errors on the estimates can be obtained by assuming that the distribution of the surface elevations is Gaussian with zero mean and a standard deviation as obtained from the profiles of the surface. Figure 2 shows a typical wave height distribution and backscattered power distribution as observed by the radar.

To test for any dependance of the EM bias (% SWH) on several surface conditions, all of the 63 combinations of SWH, skewness, kurtosis dominant wavelength, wind speed, and significant slope (Huang and Long, 1980) were used to fit the measurements to multidimensional straight lines. For each combination the standard deviation of the measured values of EM bias (% SWH) relative to the best fit line was computed. Figure 5 shows the standard deviations of the difference between the measured values of EM bias and the corresponding least squares value displayed in the order of the largest value to the smallest value. The poorest fit resulted when using SWH alone (S.D. = 1.2% SWH) and the best fit was found when all conditions were included (S.D. = 0.5% SWH). The dots along the bottom of Figure 5 show by their position the surface conditions used for a particular combination. For example in Figure 5 the line that joins the two dots in the rows of wind speed and significant slope, showing that these two conditions were used, are located directly below an upper dot indicating that the standard deviation of the fit was 0.65% SWH. There doesn't appear to be any pronounced improvement in the fit for any combination of the conditions.

Future satellite altimeter programs need to consider the EM bias as a source of error. Care should be exercised in assigning any particular value to the EM bias. Our data shows a trend in the direction of Jackson's analytical result. Our result together with (Walsh, 1982 and Hoge, 1982) indicate that the EM bias is a function of the radar wavelength. The shorter the wavelength the smaller the value of EM bias.

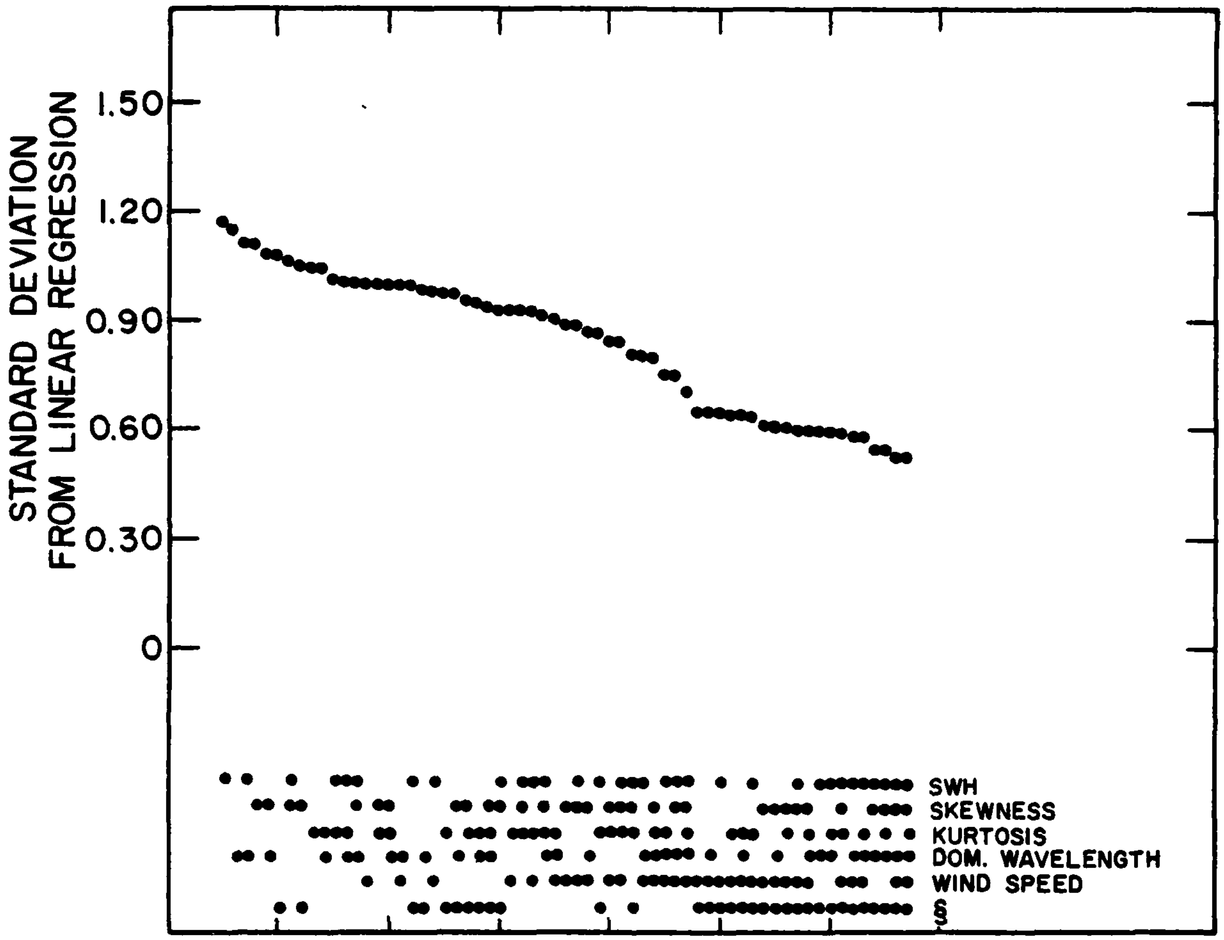

Figure 5 - Standard Deviation of EM Bias measurements from "best fit" hyperspace line. All of the 63 possible combinations of SWH, skewness, kurtosis, dominant wavelength, wind speed, and significant slope were used to fit, in a least squares sense, the measurement of EM Bias to a hyperspace line. The results are displayed in the order of highest to lowest standard deviation. The dots at the bottom show the combination used to obtain the standard deviation plotted above.

ACKNOWLEDGEMENTS

We are grateful to Dr. E. Walsh for his cooperation and support on this joint project. Special thanks to Dr. V. E. Noble for his interest and support, to Mr. R. J. Whitman II for helping with the computer programs, to Miss Marie Spangler for text editing, and preparation of the report, to Mrs. J. Ware for the illustrations, to Mr. J. R. Lewis for his help performing the field measurements, and to Dr. D. T. Chen and Dr. A. C. Miller for their technical review. This project was funded jointly by NAVAIR AIRTASK A370370G/058C/2W05270S00; ONR RR1452-SB-000, PE63371N; and NASA P-81,235(G).

REFERENCES

Born, G. H. and M. A. Richards and G. W. Rosborough, 1982, "An Empirical Determination of the Effects of Sea State Bias on SEASAT Altimetry", J. Geophys. Res., Vol. 87, No. C5, pp 3221-3226, April.

Choy, L. W. and E. A. Uliana, 1980, "Backscattering of Narrow Radar and Laser Pulses from a Non-Gaussian Sea," Terrain and Sea Scatter Workshop Proceedings, George Washington University, Washington, D. C., March.

Hoge, F. 1982, Private Communication.

Huang N. E. and S. R. Long, 1980, "An experimental Study of the Surface Elevation Probability Distribution and Statistics of Wind Generated Waves," J. Fluid Mech., 101, pp 179-200.

Jackson, F. C., 1979, "The Reflection of Impulses from a Nonlinear Random Sea," J. Geophys. Res., Vol. 84, No. C8, pp 4439-4932, August.

Kenny, J. E. and E. J. Walsh, 1978, "A Unique Radio Oceanographic Radar," NRL Memorandum Report 4086, November.

Kenny, J. E., E. A. Uliana, and E. J. Walsh, 1979, "The Surface Contour Radar, A Unique Remote Sensing Instrument," IEEE Trans. Microwave Theory and Technique, Vol. MTT-27, No. 12, December.

Lipa, B. J. and D. E. Barrick, 1980, "Ocean Surface Height-Slope Probability Density Function from SEASAT Altimeter Echo", JGR, Vol. 86, No. C11, pp 10,921-10,930, November.

Longuet-Higgins, M. S., 1963 "The Effect of Non-linearities on Statistical Distributions in the Theory of Sea Waves", Journal of Fluid Mechanics, Vol. 17, pp 459-480.

Shapiro, A., E. A. Uliana and B. S. Yaplee, 1972, NOAA Technical Report ERL 228-AOML 7, Sea Surface Topography from Space; pp 11-1 - 11-29.

Walsh, E., Private Communication.

Yaplee, B. S., A. Shapiro, D. L. Hammond, B. D. Au, and E. A. Uliana, 1971, "Nanosecond Radar Observation of the Ocean Surface from a Stable Platform," IEEE Trans. Geosci. Electron., GE-9, pp 170-174.

2-8

DT